



ELSEVIER

Polymer 43 (2002) 6871–6878

**polymer**[www.elsevier.com/locate/polymer](http://www.elsevier.com/locate/polymer)

# A study of the conformational stability of poly(L-alanine), poly(D-alanine), poly(L-isoleucine), polyglycine and poly(L-valine) and their polypeptide blends in the solid-state by $^{13}\text{C}$ CP/MAS NMR

Katsuyoshi Murata, Shigeki Kuroki, Isao Ando\*

*Department of Chemistry and Materials Science, International Research Center of Macromolecular Science,  
Tokyo Institute of Technology, 2-12-1 Ookayama, Meguro-ku, Tokyo 152-8552, Japan*

Received 15 July 2002; accepted 29 August 2002

## Abstract

$^{13}\text{C}$  CP/MAS NMR and  $^1\text{H}$   $T_{1\rho}$  experiments on homopolypeptides obtained from D- and L-alanines, L-isoleucine, glycine and L-valine, and on their polypeptide blends have been carried out, in order to elucidate the conformational stability of the polypeptides in the solid-state. These polypeptide blends were prepared by adding trifluoroacetic acid (TFA) solutions of the polypeptides containing a 2.0% (w/w) amount of sulfuric acid ( $\text{H}_2\text{SO}_4$ ) to alkaline water. From these experimental results, it was clarified that the conformations of the polypeptides in their blends are strongly influenced by intermolecular hydrogen bonding interactions which cause their miscibility at the molecular level. © 2002 Elsevier Science Ltd. All rights reserved.

*Keywords:* Conformational stability; Structure; Polypeptide; Solid state NMR

## 1. Introduction

Synthetic homopolypeptides consist of a repeated sequence of an amino acid. The structures of the homopolypeptides are not as complicated as those of proteins. Nevertheless, homopolypeptides take some specified conformations such as the  $\alpha$ -helix,  $\beta$ -sheet, etc. which appear in proteins. These individual conformations are transformed into other conformations under certain conditions such as temperature quenching. [1–7]. For example, the right-handed  $\alpha(\alpha_R)$ -helix form is transformed to the left-handed  $\alpha(\alpha_L)$ -helix form, the  $\alpha_R$ -helix form to the  $\omega$ -helix form, the  $\omega$ -helix form to the  $\beta$ -sheet form, etc. These transformations arise from the energetic stability caused by hydrogen bond (HB) interactions. Thus, according to the balance of the intra- and intermolecular HB interactions in polypeptide blends, it is expected that the strength of intermolecular interactions in the blends may be different from those in homopolypeptides such that new conformations may be formed by intermolecular interactions, which do not originally exist in the homopolypeptides.

Copolymers of alanine (Ala) and glycine (Gly) [(Ala, Gly) $_n$ ] take the right-handed  $\alpha$ -helix,  $\beta$ -sheet and  $3_1$ -helix forms in the solid-state. These are obtained by changing the composition ratio or by solvent treatment [8–11]. As well known, two kinds of synthetic polypeptides do not form polypeptide blends by using conventional method. Most recently, we have found [12] that poly(L-alanine) (PLA) and poly(L-valine) (PLV) could blend at the molecular level as prepared by adding a trifluoroacetic acid (TFA) solution of these polymers containing a 2.0% (w/w) amount of sulfuric acid ( $\text{H}_2\text{SO}_4$ ) to alkaline water. Our new method is very useful one for preparing polypeptide blends. In this work we prepare some polypeptide blends by using this method.

Hence, we have been concerned with the conformational stability of PLA/poly(L-isoleucine) (PLIL), polyglycine (PG)/PLV and poly(D-alanine) (PDA)/PLV blends. Here, let us describe some reasons why PLA/PLIL, PG/PLV and PDA/PLV blends are interesting systems. PLA and PDA in the solid-state can take the  $\alpha$ -helix and  $\beta$ -sheet forms due to intra- and intermolecular HBs, respectively. PG in the solid-state can take the  $3_1$ -helix (PG-II) and  $\beta$ -sheet (PG-I) forms due to intra- and intermolecular HBs, respectively. However, PLIL and PLV in the solid-state can predominantly take the  $\beta$ -sheet form as the stable conformation. For this

\* Corresponding author. Tel.: +81-3-5734-2139; fax: +81-3-5734-2889.  
E-mail address: iando@polymer.titech.ac.jp (I. Ando).

reason, it is interesting to know whether an isolated  $\alpha$ -helix or  $3_1$ -helix polypeptide surrounded by a major polypeptide in the  $\beta$ -sheet form can take the helical conformation or not. In addition, we would like to know whether a polypeptide in the  $\beta$ -sheet form surrounded by a major polypeptide in the  $\alpha$ -helix or  $3_1$ -helix form can take the  $\beta$ -sheet conformation. By using their blended systems, such a conformational change may provide some useful knowledge about the conformational stability. The balance of intra- and inter-molecular HB interactions would also play a role.

As an NMR methodology for elucidating conformational stability in the PLA/PLIL, PG/PLV and PDA/PLV systems, the conformation-dependent  $^{13}\text{C}$  NMR chemical shift for polypeptides in the solid-state is used in this work. This approach has been demonstrated in a series of previous works [13–18] as described below. It has been elucidated that the  $^{13}\text{C}$  NMR chemical shifts of a number of polypeptides and proteins in the solid-state, as determined by the CP/MAS (cross-polarization/magic angle spinning) method, are significantly displaced, depending on their particular conformations such as  $\alpha$ -helix,  $3_1$ -helix or  $\beta$ -sheet [13–21].

In this work, therefore, we aim to prepare PLA/PLIL, PG/PLV and PDA/PLV blend samples with various mixture ratios and to elucidate the conformational stability of their polypeptides and their blended samples by  $^{13}\text{C}$  CP/MAS NMR and  $^1\text{H}$   $T_{1\rho}$  experiments.

## 2. Experimental

### 2.1. Materials

Poly(L-alanine) (molecular weight,  $M_w$ : 23 600) in the right-handed  $\alpha$ -helix form, poly(D-alanine) ( $M_w$ : 3000) in the left-handed  $\alpha$ -helix form, poly(L-isoleucine) ( $M_w$ : 8500) in the  $\beta$ -sheet form, poly(L-valine) ( $M_w$ : 1700–1900) in the  $\beta$ -sheet form and polyglycine ( $M_w$ : 1000) in the  $\beta$ -sheet form (PG-I) were purchased from Sigma Chemical Co., respectively [13–15]. Polyglycine in the  $3_1$ -helix (PG-II) form was obtained by precipitation from an aqueous lithium bromide (LiBr) solution of PG [8–10]. Poly(L-alanine) ( $M_w$ : 1000–5000) with a 1/1 mixture of the  $\beta$ -sheet and  $\alpha$ -helix forms, as determined by  $^{13}\text{C}$  CP/MAS NMR was purchased from Sigma Chemical Co. As reported previously [22], low molecular weight PLA takes the  $\beta$ -sheet form. The conformation of these polypeptides was checked by  $^{13}\text{C}$  CP/MAS NMR. The polypeptide mixtures with various ratios of 100/0, 80/20, 50/50, 20/80, and 0/100% (w/w) were dissolved in trifluoroacetic acid with 2.0% (w/w) amount of  $\text{H}_2\text{SO}_4$ , which is the ‘random coil’ solvent [23] for these polypeptides. Their solutions were added to alkaline water at room temperature and the precipitated blend samples were washed with water and dried under vacuum at 308–318 K.

### 2.2. Measurements

$^{13}\text{C}$  CP/MAS NMR measurements were performed on a Bruker DSX-300 spectrometer operating at 75 MHz equipped with a CP/MAS accessory at room temperature. The  $^1\text{H}$   $90^\circ$  pulse width was 3.7  $\mu\text{s}$ , the contact time was 2 ms, and the pulse delay was 5 s. The spectral width and number of data points were 27 kHz and 2k, respectively. Samples were placed in a bullet-type rotor and spun at 5–7 kHz. Spectra were accumulated 144–520 times to achieve a reasonable signal-to-noise ratio. The  $^{13}\text{C}$  chemical shifts were calibrated indirectly through the low frequency adamantane peak (29.5 ppm relative to tetramethylsilane).

The spin–lattice relaxation times in the rotating frame for protons ( $^1\text{H}$   $T_{1\rho}$ ) were obtained by the standard CP scheme. For the  $^1\text{H}$   $T_{1\rho}$  measurements we used a spin-lock sequence with various spin-locking times ( $\tau$ ). The  $^1\text{H}$   $90^\circ$  pulse width used in the spin-locking experiments is 3.7  $\mu\text{s}$ . The proton data are detected through carbon by the CP process. The contact time was set to 2 ms and  $^1\text{H}$  spin-locking times were changed in the range of 0.01–10 ms. The  $^1\text{H}$   $T_{1\rho}$  is very sensitive to the domain size of individual polymers in polymer blends through the spin-diffusion process. Therefore, this method becomes very useful for the study of miscibility in polymer blends [24].

As reported in previous papers [25–28] the fractions of  $\alpha$ -helical and  $\beta$ -sheet conformations of the L-Ala residue in various polypeptides in the solid-state can be determined by  $^{13}\text{C}$  CP/MAS measurements. These include the dipolar dephasing time,  $^{13}\text{C}$   $T_1$  and  $^1\text{H}$   $T_{1\rho}$  experiments and the CP efficiency experiments on various polypeptide mixtures.

## 3. Results and discussion

### 3.1. $^{13}\text{C}$ CP/MAS NMR spectra and conformational characterization

(1) *PLA/PLIL blend sample.* The observed  $^{13}\text{C}$  CP/MAS NMR spectra of PLA, PLIL and the PLA/PLIL (50/50) blend samples as prepared by adding a TFA solution of PLA, PLIL and a mixture of PLA/PLIL with a 2.0% (w/w) amount of  $\text{H}_2\text{SO}_4$  to alkaline water are shown in Fig. 1. The assignments of these spectra are made by the above-mentioned method. The  $^{13}\text{C}$  chemical shift values of these polypeptide samples are listed together with the reference data of PLA in the right-handed  $\alpha$ -helix form and  $\beta$ -sheet form, and PLIL in the  $\beta$ -sheet form [22,29,30] in Table 1. The reference  $^{13}\text{C}$  chemical shift data were used for the conformational characterization as shown below. The three intense peaks at 176.9, 53.3 and 15.5 ppm which appear in the spectrum of PLA (Fig. 1(a)) can be assigned to the C=O, C $\alpha$ , and C $\beta$  carbons, respectively. From these  $^{13}\text{C}$  chemical shift values, it is found that the PLA used in this work takes the  $\alpha$ -helix form. There are no peaks which come from the  $\beta$ -sheet form. On the other hand, in the spectrum of PLIL

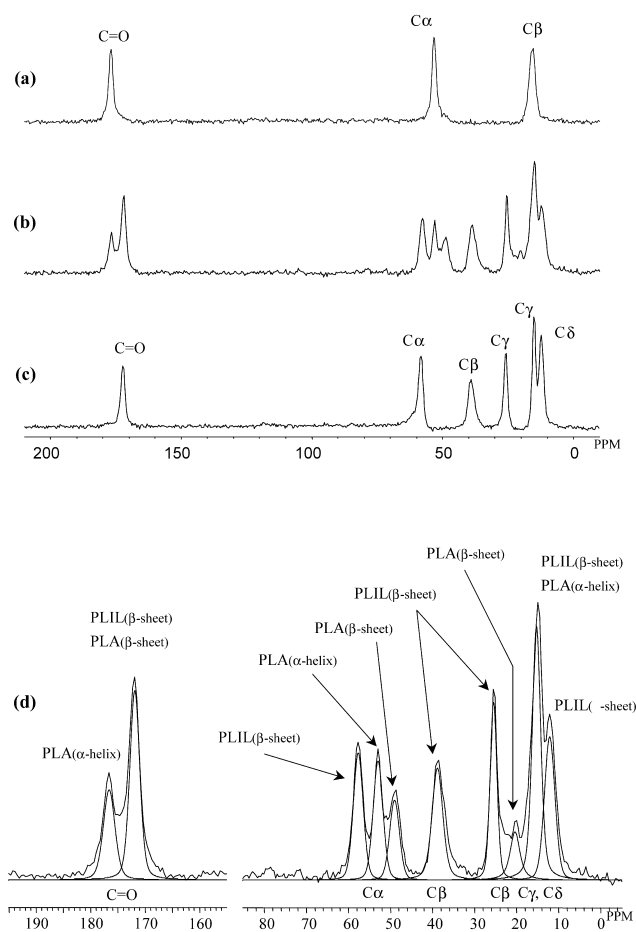


Fig. 1.  $^{13}\text{C}$  CP/MAS NMR spectra of the PLA, PLIL and PLA/PLIL blend samples. (a) PLA/PLIL (100/0), (b) PLA/PLIL (50/50), (c) PLA/PLIL (0/100) and (d) expanded  $^{13}\text{C}$  CP/MAS NMR spectrum for the carbonyl carbon region and for the  $\text{C}\alpha$ ,  $\text{C}\beta$ ,  $\text{C}\gamma$  and  $\text{C}\delta$  carbon regions of the PLA/PLIL blend with the mixture ratio of 50/50% (w/w).

(Fig. 1(c)), the six intense peaks appear at 172.0, 58.1, 39.6, 25.9/15.0 and 12.3 ppm and can be assigned to the  $\text{C}=\text{O}$ ,  $\text{C}\alpha$ ,  $\text{C}\beta$ ,  $\text{C}\gamma/\text{C}\gamma$ , and  $\text{C}\delta$  carbons, respectively. From these  $^{13}\text{C}$  chemical shift values, it is found that PLIL takes the  $\beta$ -sheet form.

Next, we are concerned with the conformational characterization of the PLA/PLIL blends. The observed  $^{13}\text{C}$  CP/MAS NMR spectrum for a PLA/PLIL blend sample with a mixture ratio of 50/50% (w/w) is shown in Fig. 1(b), which corresponds to the molar mixture ratio of ( $= 1.60$ ). In the  $^{13}\text{C}$  CP/MAS spectrum, a new peak for the  $\text{C}\alpha$  carbon of PLA appears clearly at 48.9–49.2 ppm. This peak can be assigned to the  $\text{C}\alpha$  carbon of PLA in the  $\beta$ -sheet form. In order to clarify in detail the appearance of this new peak, the  $\text{C}=\text{O}$  carbon region and the  $\text{C}\alpha$ ,  $\text{C}\beta$ ,  $\text{C}\gamma$  and  $\text{C}\delta$  carbon regions in the spectrum of the PLA/PLIL blend with a mixture ratio of 50/50% (w/w), were expanded as shown in Fig. 1(d). By computer-fitting the observed spectrum was decomposed as a sum of Lorentzian lineshapes, and then the fractions of the  $\alpha$ -helix and  $\beta$ -sheet forms for PLA and PLIL

Table 1

Observed solid-state  $^{13}\text{C}$  chemical shifts of PLA, PLIL and PLA/PLIL blend samples

Polypeptide samples	$^{13}\text{C}$ chemical shift (ppm)					Conformation
	$\text{C}=\text{O}$	$\text{C}\alpha$	$\text{C}\beta$	$\text{C}\gamma$	$\text{C}\delta$	
PLA	176.7	53.2	16.0			$\alpha$ -Helix <sup>a</sup>
PLA	172.4	49.4	20.7			$\beta$ -Sheet <sup>a</sup>
PLIL	172.0	58.0	38.6	25.9/15.0	12.0	$\beta$ -Sheet <sup>a</sup>
PLA/PLIL (100/0)	176.9	53.3	15.5			PLA $\alpha$ -helix
PLA/PLIL (80/20)	176.7	53.2	15.5			PLA $\alpha$ -helix
	172.1	49.2	20.3			PLA $\beta$ -sheet
	– <sup>b</sup>	58.1	38.8	25.7/– <sup>b</sup>	12.2	PLIL $\beta$ -sheet
PLA/PLIL (50/50)	176.7	53.2	– <sup>b</sup>			PLA $\alpha$ -helix
	– <sup>b</sup>	49.1	20.5			PLA $\beta$ -sheet
	172.1	58.0	38.7	25.6/15.2	12.4	PLIL $\beta$ -sheet
PLA/PLIL (20/80)	176.7	53.2	– <sup>b</sup>			PLA $\alpha$ -helix
	– <sup>b</sup>	48.9	20.3			PLA $\beta$ -sheet
	172.1	58.0	39.2	25.7/15.0	12.3	PLIL $\beta$ -sheet
PLA/PLIL (0/100)	172.0	58.1	39.6	25.9/15.0	12.3	PLIL $\beta$ -sheet

<sup>a</sup> Refs. [22,29,30].

<sup>b</sup> Not determined because of the overlap of the minor peak with the major peak.

were determined. The determined ( $\alpha$ -helix form +  $\beta$ -sheet form) peak intensity for the  $\text{C}\alpha$  carbons of PLA ( $f_{\text{PLA}}$ ) is much larger than that for the  $\text{C}\alpha$  carbons of PLIL in the  $\beta$ -sheet form ( $f_{\text{PLIL}}$ ). Then, the ratio of  $f_{\text{PLA}}/f_{\text{PLIL}}$  is about 1.61. This is very close to theoretical prediction of 1.60. This means that the fractions of the  $\alpha$ -helix and  $\beta$ -sheet form can be estimated by  $^{13}\text{C}$  CP/MAS NMR. Another new peak of the  $\text{C}\beta$  carbon of PLA appears at about 20.5 ppm, in addition to an intense peak assigned to the  $\alpha$ -helix form (16.0 ppm), and this can be assigned to the  $\beta$ -sheet form (20.5 ppm). These results show that the  $\alpha$ -helix form of PLA in PLA/PLIL blends is partially transformed to the  $\beta$ -sheet form.

(2) PG/PLV blend sample. The observed  $^{13}\text{C}$  CP/MAS NMR spectra of PG, PLV and the PG/PLV (50/50) blend samples are shown in Fig. 2. The assignments of these spectra were made by the above-mentioned method. The  $^{13}\text{C}$  chemical shift values of these polypeptide samples are listed together with those for PG in the  $3_1$ -helix form (PG-II) and  $\beta$ -sheet form (PG-I), and PLV in the  $\beta$ -sheet form [22, 29,30] in Table 2. The two intense peaks at 172.9 and 42.9 ppm, which appear in the spectrum of PG (Fig. 2(a)) can be assigned to the  $\text{C}=\text{O}$  and  $\text{C}\alpha$  carbons. From these  $^{13}\text{C}$  chemical shift values, it is found that the PG used in this work takes the  $3_1$ -helix form. There are no peaks which come from the  $\beta$ -sheet form. On the other hand, in the spectrum of PLV (Fig. 2(c)), the four intense peaks appear at 172.0, 58.6, 32.8 and 19.0 ppm and can be assigned to the  $\text{C}=\text{O}$ ,  $\text{C}\alpha$ ,  $\text{C}\beta$  and  $\text{C}\gamma$  carbons, respectively. From these  $^{13}\text{C}$  chemical shift values, it is found that PLV takes the  $\beta$ -sheet form.

Next, we are concerned with the conformational characterization of PG/PLV blends. The observed  $^{13}\text{C}$  CP/MAS NMR spectrum for the PG/PLV (50/50) blend

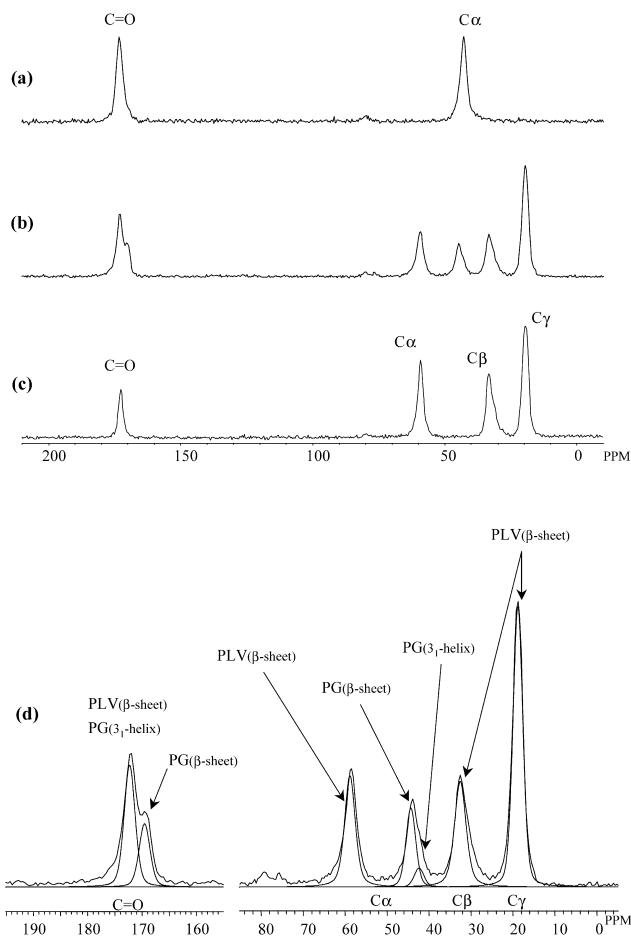


Fig. 2.  $^{13}\text{C}$  CP/MAS NMR spectra of the PG, PLV and PG/PLV blend samples. (a) PG/PLV (100/0), (b) PG/PLV (50/50), (c) PG/PLV (0/100) and (d) expanded  $^{13}\text{C}$  CP/MAS NMR spectrum for the carbonyl carbon region and for the  $\text{C}\alpha$ ,  $\text{C}\beta$  and  $\text{C}\gamma$  carbon regions of the PG/PLV blend with the mixture ratio of 50/50% (w/w).

sample is shown in Fig. 2(b). In the  $^{13}\text{C}$  CP/MAS spectrum, a new peak for the  $\text{C}=\text{O}$  carbon appears clearly at 169.5–169.9 ppm. This peak can be assigned to the  $\text{C}=\text{O}$  carbon of PG in the  $\beta$ -sheet form as seen from Table 2. In order to clarify in detail the appearance of this new peak, the carbonyl carbon region and the  $\text{C}\alpha$ ,  $\text{C}\beta$  and  $\text{C}\gamma$  carbon region in the spectrum of the PG/PLV blend, with a mixture ratio of 50/50%, were expanded as shown in Fig. 2(d). By computer-fitting the observed spectrum was decomposed, and then the fractions of the  $3_1$ -helix and  $\beta$ -sheet forms for PG and PLV were determined.

Another new peak of the  $\text{C}\alpha$  carbon of PG appears at about 44.3 ppm in addition to a small peak assigned to the  $3_1$ -helix form (42.6 ppm), and can be assigned to the  $\beta$ -sheet form (44.3 ppm). These results show that the  $3_1$ -helix form of PG in the PG/PLV blends is partially transformed to the  $\beta$ -sheet form.

(3) PDA/PLV blend sample. The observed  $^{13}\text{C}$  CP/MAS NMR spectra of PDA, PLV and a PDA/PLV (50/50) blend sample are shown in Fig. 3. The assignments of these spectra are made by the above-mentioned method. The  $^{13}\text{C}$

Table 2  
Observed solid-state  $^{13}\text{C}$  chemical shifts of PG, PLV and PG/PLV blend samples

Polypeptide samples	$^{13}\text{C}$ chemical shift (ppm)				Conformation
	$\text{C}=\text{O}$	$\text{C}\alpha$	$\text{C}\beta$	$\text{C}\gamma$	
PG	172.9	42.6			$3_1$ -Helix <sup>a</sup>
PG	169.0	44.3			$\beta$ -Sheet <sup>a</sup>
PLV	172.3	58.6	32.9	19.0	$\beta$ -Sheet <sup>a</sup>
PG/PLV (100/0)	172.9	42.9			PG $3_1$ -helix
PG/PLV (80/20)	172.5	42.8			PG $3_1$ -helix
	169.5	44.0			PG $\beta$ -sheet
PG/PLV (50/50)	– <sup>b</sup>	58.6	32.7	19.1	PLV $\beta$ -sheet
	– <sup>b</sup>	42.8			PG $3_1$ -helix
	169.5	44.3			PG $\beta$ -sheet
PG/PLV (20/80)	172.2	58.9	32.9	19.0	PLV $\beta$ -sheet
	– <sup>b</sup>	42.8			PG $3_1$ -helix
	169.9	44.5			PG $\beta$ -sheet
PG/PLV (0/100)	172.2	58.8	33.0	19.0	PLV $\beta$ -sheet
	172.0	58.6	32.8	19.0	PLV $\beta$ -sheet

<sup>a</sup> Refs. [22,29,30].

<sup>b</sup> Not determined because of the overlap of the minor peak with the major peak.

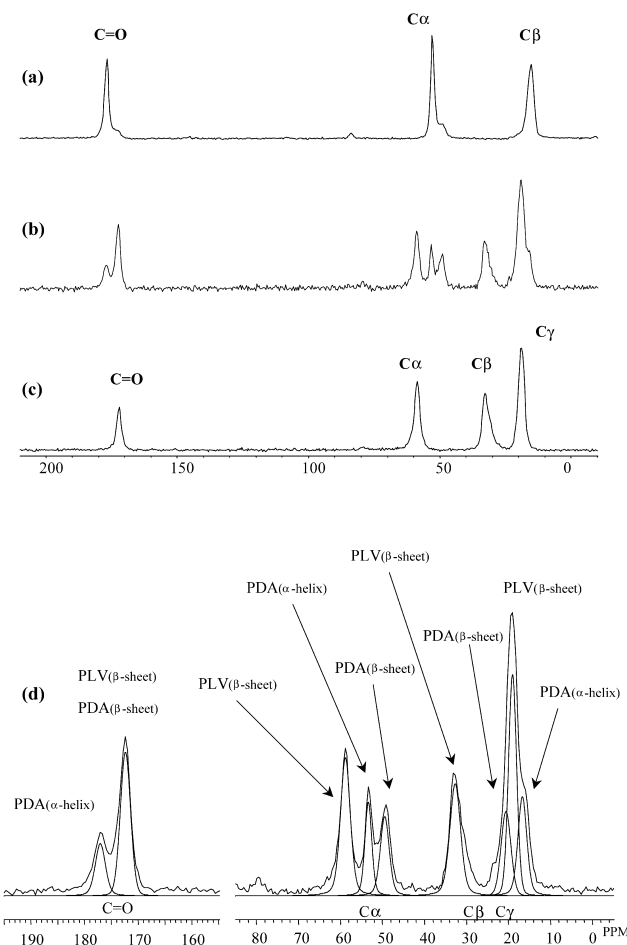


Fig. 3.  $^{13}\text{C}$  CP/MAS NMR spectra of the PDA, PLV and PDA/PLV blend samples. (a) PDA/PLV (100/0), (b) PDA/PLV (50/50), (c) PDA/PLV (0/100) and (d) expanded  $^{13}\text{C}$  CP/MAS NMR spectrum for the carbonyl carbon region and for the  $\text{C}\alpha$ ,  $\text{C}\beta$  and  $\text{C}\gamma$  carbon regions of the PDA/PLV blend with the mixture ratio of 50/50% (w/w).

Table 3  
Observed solid-state  $^{13}\text{C}$  chemical shifts of PDA, PLV and PDA/PLV blend samples

Polypeptide samples	$^{13}\text{C}$ chemical shift (ppm)				Conformation
	C=O	C $\alpha$	C $\beta$	C $\gamma$	
PDA <sup>b</sup>	176.8	53.1	15.7		$\alpha$ -Helix <sup>a</sup>
PLA	172.4	49.4	20.7		$\beta$ -Sheet <sup>a</sup>
PLV	172.3	58.6	32.9	19.0	$\beta$ -Sheet <sup>a</sup>
PDA/PLV (100/0)	176.6	53.3	15.7		PDA $\alpha$ -helix
PDA/PLV (50/50)	176.8	53.1	15.9		PDA $\alpha$ -helix
	– <sup>c</sup>	48.9	20.9		PDA $\beta$ -sheet
	172.2	58.6	32.7	19.0	PLV $\beta$ -sheet
PDA/PLV (0/100)	172.2	58.9	32.9	19.0	PLV $\beta$ -sheet

<sup>a</sup> Refs. [22,29,30].

<sup>b</sup> Very small  $\beta$ -sheet C=O and C $\alpha$  peaks appear at ca. 172 and 49 ppm, respectively, as a broad shoulder of an intense  $\alpha$ -helix peak. Therefore, it is difficult to obtain the exact chemical shift values of the PDA  $\beta$ -sheet form. As the chemical shift values of PDA  $\beta$ -sheet form, the chemical shift values of PLA  $\beta$ -sheet form are shown instead of PDA as reference data.

<sup>c</sup> Not determined because of the overlap of the minor peak with the major peak.

chemical shift values of these polypeptide samples are listed in Table 3 together with the reference data of PDA in the  $\alpha$ -helix form and PLA and PLV in the  $\beta$ -sheet form [22,29,30]. Very small  $\beta$ -sheet C=O and C $\alpha$  peaks appear at ca. 172 and 49 ppm, respectively, as a broad shoulder of an intense  $\alpha$ -helix peak. Therefore, it is difficult to obtain the exact chemical shift values of the PDA  $\beta$ -sheet form. However, the chemical shift values of the PLA  $\beta$ -sheet form may be the same as those of PDA. The three intense peaks at 176.6, 53.3 and 15.7 ppm which appear in the spectrum of PDA (Fig. 3(a)) can be assigned to the C=O, C $\alpha$  and C $\beta$  carbons, respectively. From these  $^{13}\text{C}$  chemical shift values, it is found that the PDA used in this work takes the  $\alpha$ -helix form. On the other hand, in the spectrum of PLV (Fig. 3(c)), the four intense peaks appear at 172.2, 58.9, 32.9 and 19.0 ppm, and can be assigned to the C=O, C $\alpha$ , C $\beta$ , and C $\gamma$  carbons, respectively. From these  $^{13}\text{C}$  chemical shift values, it is found that PLV takes the  $\beta$ -sheet form.

We are concerned with the conformational characterization of PDA/PLV blends. The observed  $^{13}\text{C}$  CP/MAS NMR spectrum for the PDA/PLV (50/50) blend sample is shown in Fig. 3(b). In the  $^{13}\text{C}$  CP/MAS spectrum, a new peak for the C $\alpha$  carbon of PDA appears clearly at 48.9 ppm. This peak can be assigned to the C $\alpha$  carbon of PDA in the  $\beta$ -sheet form. In order to clarify in detail the appearance of this new peak, the carbonyl carbon region and the C $\alpha$ , C $\beta$  and C $\gamma$  carbon regions in the spectrum of the PDA/PLV (50/50) blend sample were expanded as shown in Fig. 3(d). By computer-fitting the observed spectrum was decomposed, and then the fractions of the  $\alpha$ -helix and  $\beta$ -sheet forms for PDA and PLV were determined. Another new peak of the C $\beta$  carbon of PDA appears at about 20.9 ppm, in addition to an intense peak assigned to the  $\alpha$ -helix form (15.7 ppm), and this can be assigned to the  $\beta$ -sheet form (20.9 ppm).

These results show that the  $\alpha$ -helix form of PDA in the PDA/PLV blends is partially transformed to the  $\beta$ -sheet form.

From the above results, it is very significant to realize that the homopolypeptides of PLA, PDA and PG in the helix form do not form the  $\beta$ -sheet form used by the TFA-alkaline treatment for preparing blend samples. However, the conformation of their blend samples, prepared by the TFA-alkaline treatment, is changed from the  $\alpha$ -helix or  $3_1$ -helix form to the  $\beta$ -sheet form. Further, it can be said that the  $\beta$ -sheet form of PLA, PDA and PG in the blend polymers is incorporated into PLIL and PLV in the  $\beta$ -sheet form. It then takes the  $\beta$ -sheet form by forming hydrogen bonds with PLIL and PLV, and the other components of PLA, PDA and PG take the helix form. Thus, we can say that the generation of the conformation of PLA, PDA and PG in PLA/PLIL, PDA/PLV and PG/PLV blends may be closely associated with changes in the strength of intermolecular HB interactions between the polypeptides.

Such a conclusive consideration is certainly speculative. Nevertheless, we think that it may be acceptable because of our detailed analysis of the experimental data. When each of PLA, PDA, PG, PLIL and PLV samples was treated under the same treatment condition as the individual case of their blends as described above, the structure of polypeptides after its treatment did not change from the original structure as seen from the  $^{13}\text{C}$  CP/MAS NMR experiments. On the other hand, the structure of blended polypeptides after the treatment significantly changes. Therefore, it can be said that such a change comes from intermolecular interactions of them.

$^1\text{H}$   $T_{1\rho}$  Experiments on PLA, PLIL, PG, PDA, PLV, PLA/PLIL, PG/PLV and PDA/PLV blend with a mixture ratio of 50/50 and the blend compatibility. The  $^1\text{H}$   $T_{1\rho}$  data are sensitive to the domain size of individual polymers in polymer blends through the spin-diffusion process and thus can be used to study the miscibility of polymer blends. Since the efficiency of spin-diffusion is governed by dipole–dipole interactions, knowledge of the rate of spin-diffusion among proton spins of individual polymers in polymer blends would provide useful information about domain sizes in the region of 2–5 nm [24,31–35]. Therefore, more detailed information about the structure of PLA/PLIL, PG/PLV and PDA/PLV blends can be obtained by the  $^1\text{H}$   $T_{1\rho}$  experiments. Typical  $^{13}\text{C}$  CP/MAS NMR spectra of PLA/PLIL (50/50), PG/PLV (50/50) and PDA/PLV (50/50) blend samples are measured as a function of  $^1\text{H}$  spin-locking time,  $\tau$  (not shown). In the PG/PLV blend spectrum two peaks for the PG C $\alpha$  carbon in the  $3_1$ -helix form and  $\beta$ -sheet form are overlapping with each other as shown in Fig. 3. For this reason, we used computer-fitting method to determine the  $^1\text{H}$   $T_{1\rho}$  value as exactly as possible. We think that although the experimental error is somewhat larger compared with the results determined from two separated peaks, its value may be used in discussion of the polymer blends. The intensities of the individual peaks decrease with an increase

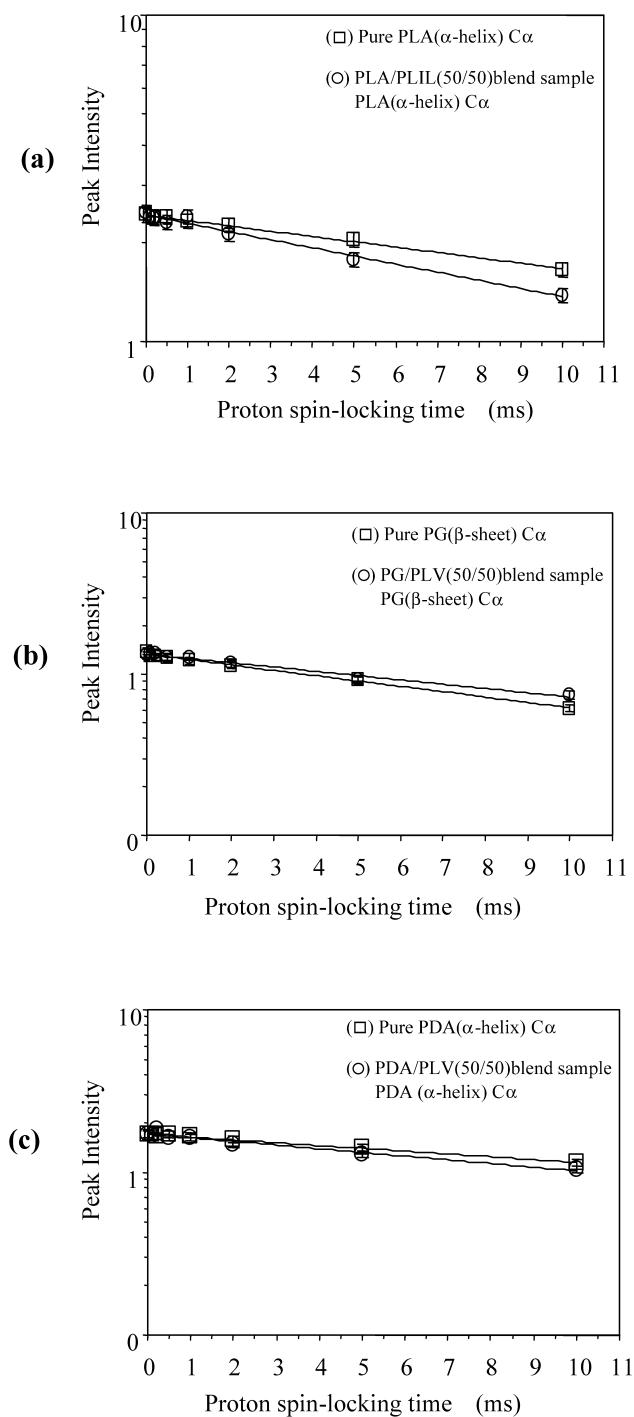


Fig. 4. Typical semi-log plots of the peak intensities for the reference and blend samples against the proton spin-locking time  $\tau$ . (a) PLA/PLIL (50/50), (b) PG/PLV (50/50) and (c) PDA/PLV (50/50).

in  $\tau$ . The semi-log plot of the peak intensities for the individual carbons of the blend samples, against  $\tau$ , becomes a straight line and from its slope the  ${}^1\text{H } T_{1\rho}$  value is obtained. As a typical example, it is convenient to show the semi-log plot of the peak intensity of the  $\text{C}\alpha$  carbon against the spin-locking time  $\tau$  in the  ${}^1\text{H } T_{1\rho}$  experiments on

Table 4

Determined  ${}^1\text{H } T_{1\rho}$  values of PLA, PLIL and PLA/PLIL (50/50) blend samples

Polypeptide samples	${}^1\text{H } T_{1\rho}$ (ms)					Conformation
	C=O	C $\alpha$	C $\beta$	C $\gamma$	C $\delta$	
PLA	27	27	26			$\alpha$ -Helix
PLA	21	19	20			$\beta$ -Sheet
PLIL	11	11	11	12/11	11	$\beta$ -Sheet
PLA/PLIL (50/50)	16	17	– <sup>a</sup>			PLA $\alpha$ -helix
	– <sup>a</sup>	17	19			PLA $\beta$ -sheet
	12	14	13	14/14	14	PLIL $\beta$ -sheet

<sup>a</sup> Not determined because of the overlap of the minor peak with the major peak.

homopolypeptides and their blend samples in Fig. 4(a–c), in order to elucidate molecular motion as mentioned below.

(1) *PLA/PLIL (50/50) blend sample*. It is clear that there are significant differences between the two slopes of the semi-log plots for the  $\text{C}\alpha$  carbon of pure PLA with the  $\alpha$ -helix form and the  $\text{C}\alpha$  carbon of PLA in the  $\alpha$ -helix form in the PLA/PLIL (50/50) blend sample (Fig. 4(a)), and the experimental error is within  $\pm 5\%$ . From these plots, we can obtain the  ${}^1\text{H } T_{1\rho}$  values of 27 and 17 ms for these samples, respectively. Similarly, we can obtain the significant  ${}^1\text{H } T_{1\rho}$  values for PLA and PLIL in the PLA/PLIL (50/50) samples. All of the  ${}^1\text{H } T_{1\rho}$  values of PLA, PLV, and the PLA/PLIL (50/50) samples are shown in Table 4. The  ${}^1\text{H } T_{1\rho}$  values for the  $\text{C}\beta$  and the  $\text{C}=\text{O}$  carbons of the PLA/PLIL (50/50) blend indicated by *a*, could not be determined because of the overlap of the minor  $\text{C}\beta$  (PLA:  $\alpha$ -helix) peak with the major  $\text{C}\gamma$  (PLIL) peak and the minor  $\text{C}=\text{O}$  (PLA:  $\beta$ -sheet) peak with the major  $\text{C}=\text{O}$  (PLIL) peak as determined by computer-fitting.

The  ${}^1\text{H } T_{1\rho}$  values determined from the  $\text{C}\alpha$ ,  $\text{C}\beta$  and  $\text{C}=\text{O}$  carbon signals of pure PLA in the  $\alpha$ -helix form are 27, 26 and 27 ms, respectively, and those of the PLA (mixture of the  $\beta$ -sheet and  $\alpha$ -helix forms, 1:1) with the  $\beta$ -sheet form are 19, 20 and 21 ms, respectively. On the other hand, the  ${}^1\text{H } T_{1\rho}$  values determined from the  $\text{C}\alpha$ ,  $\text{C}\beta$ ,  $\text{C}\gamma$ ,  $\text{C}\delta$  and  $\text{C}=\text{O}$  carbons of pure PLIL in the  $\beta$ -sheet form are 11, 11, 12/11, 11 and 11 ms, respectively. The  ${}^1\text{H } T_{1\rho}$  values for PLA in the  $\beta$ -sheet form are larger than those for PLIL in the  $\beta$ -sheet form. However, the  ${}^1\text{H } T_{1\rho}$  values for PLA in the  $\alpha$ -helix form are much larger than those for PLA and PLIL in the  $\beta$ -sheet form. In PLA/PLIL (50/50) blend, the  ${}^1\text{H } T_{1\rho}$  values determined from the  $\text{C}\alpha$ ,  $\text{C}\beta$ ,  $\text{C}\gamma$  and  $\text{C}\delta$  carbons of PLIL in the  $\beta$ -sheet form are 14, 13, 14/14 and 14 ms, respectively, and are thus slightly larger than those for pure PLIL. The  ${}^1\text{H } T_{1\rho}$  values determined from the  $\text{C}\alpha$  and  $\text{C}\beta$  carbons of PLA in the  $\beta$ -sheet form are 17 and 19 ms, respectively, and the  $\text{C}\alpha$  carbon of PLA in the  $\alpha$ -helix form is 17 ms. Hence, these  ${}^1\text{H } T_{1\rho}$  values are very close to each other. This shows that proton spin-diffusion between the PLAs in the  $\alpha$ -helix and  $\beta$ -sheet forms and PLIL in the  $\beta$ -sheet form occurs on the  ${}^1\text{H } T_{1\rho}$  time scale.

Table 5  
Determined  $^1\text{H } T_{1\rho}$  values of PG, PLV and PG/PLV (50/50) blend samples

Polypeptide samples	$^1\text{H } T_{1\rho}$ (ms)				Conformation
	C=O	C $\alpha$	C $\beta$	C $\gamma$	
PG	17	18			3 <sub>1</sub> -Helix
PG	13	13			$\beta$ -Sheet
PLV	19	19	18	18	$\beta$ -Sheet
PG/PLV (50/50)	– <sup>a</sup>	15			PG 3 <sub>1</sub> -helix
	16	16			PG $\beta$ -sheet
	13	14	14	12	PLV $\beta$ -sheet

<sup>a</sup> Not determined because of the overlap of the minor peak with the major peak.

(2) *PG/PLV (50/50) blend sample*. From Fig. 4(b), it can be obtained that the C $\alpha$  carbon of pure PG in the  $\beta$ -sheet form and the C $\alpha$  carbon of PG in the  $\beta$ -sheet form in the PG/PLV (50/50) blend sample are 13 and 16 ms, respectively. Similarly, we can obtain the significant  $^1\text{H } T_{1\rho}$  values for PG and PLV in the PG/PLV (50/50) sample. All of the determined  $^1\text{H } T_{1\rho}$  values of PGs, PLV and PG/PLV (50/50) samples are shown in Table 5, where the  $^1\text{H } T_{1\rho}$  value for the C=O carbon of PG/PLV (50/50) indicated by *a* could not be determined because of the overlap of the minor C=O (PG: 3<sub>1</sub>-helix) peak with the major C=O (PLV:  $\beta$ -sheet) peak as determined by computer-fitting.

The  $^1\text{H } T_{1\rho}$  values determined from the C $\alpha$  and C=O carbon signals of pure PG in the  $\beta$ -sheet form are 13 and 13 ms, respectively, and those for pure PG in the 3<sub>1</sub>-helix form are 18 and 17 ms, respectively. On the other hand, the  $^1\text{H } T_{1\rho}$  values determined from the C $\alpha$ , C $\beta$ , C $\gamma$  and C=O carbons of pure PLV in the  $\beta$ -sheet form are 19, 18, 18 and 19 ms, respectively. The  $^1\text{H } T_{1\rho}$  values for PG in the 3<sub>1</sub>-helix form are larger than those of PG in the  $\beta$ -sheet form, and are somewhat smaller than those of PLV in the  $\beta$ -sheet form. In the PG/PLV (50/50) blend, the  $^1\text{H } T_{1\rho}$  values determined from the C $\alpha$  C $\beta$  and C $\gamma$  carbons of PLV in the  $\beta$ -sheet form are 14, 14 and 12 ms, respectively, and are smaller than those for pure PLV. The  $^1\text{H } T_{1\rho}$  value determined from the C $\alpha$  carbon of PG in the 3<sub>1</sub>-helix form is 15 ms, and that from

Table 6  
Determined  $^1\text{H } T_{1\rho}$  values of PDA, PLV and PDA/PLV (50/50) blend samples

Polypeptide samples	$^1\text{H } T_{1\rho}$ (ms)				Conformation
	C=O	C $\alpha$	C $\beta$	C $\gamma$	
PDA	26	25	26		$\alpha$ -Helix
PLA <sup>a</sup>	21	19	20		$\beta$ -Sheet
PLV	19	19	18	18	$\beta$ -Sheet
PDA/PLV (50/50)	17	20	19		PDA $\alpha$ -helix
	– <sup>b</sup>	18	17		PDA $\beta$ -sheet
	18	16	16	16	PLV $\beta$ -sheet

<sup>a</sup> As the  $^1\text{H } T_{1\rho}$  values of PDA  $\beta$ -sheet form have not been reported, the  $^1\text{H } T_{1\rho}$  values of PLA  $\beta$ -sheet form have been shown instead of PDA.

<sup>b</sup> Not determined because of the overlap of the minor peak with the major peak.

the C $\alpha$  carbon of PG in the  $\beta$ -sheet form is 16 ms. These values are approximately equal to each other. This shows that proton spin-diffusion, between the PGs in the 3<sub>1</sub>-helix and  $\beta$ -sheet forms and PLV in the  $\beta$ -sheet form, occurs on the  $^1\text{H } T_{1\rho}$  time scale.

(3) *PDA/PLV (50/50) blend sample*. As shown in Fig. 4(c), it is clear that there are significant differences between the two slopes of the semi-log plots for the C $\alpha$  carbon of pure PDA in the  $\alpha$ -helix form and the C $\alpha$  carbon of PDA in the  $\alpha$ -helix form in the PDA/PLV (50/50) blend. From these slopes, we can obtain the  $^1\text{H } T_{1\rho}$  values of 25 and 20 ms for them, respectively. Similarly, we can obtain the significant  $^1\text{H } T_{1\rho}$  values for PDA and PLV in the PDA/PLV (50/50) samples. All of the determined  $^1\text{H } T_{1\rho}$  values of the PDA, PLV, and PDA/PLV (50/50) samples are shown in Table 6, where the  $^1\text{H } T_{1\rho}$  value of the C=O carbon of PDA/PLV (50/50) indicated by *b* could not be determined because of the overlap of the minor C=O (PDA:  $\beta$ -sheet) peak with the major C=O (PLV) peak as determined by computer-fitting. The  $^1\text{H } T_{1\rho}$  values of the PDA  $\beta$ -sheet form are not known. However, the  $^1\text{H } T_{1\rho}$  values of the PLA  $\beta$ -sheet form may be the same as those of PDA.

The  $^1\text{H } T_{1\rho}$  values determined from the C $\alpha$ , C $\beta$  and C=O carbon signals of pure PDA in the  $\alpha$ -helix form are 25, 26 and 26 ms, respectively, and those of the PLA (mixture of the  $\beta$ -sheet and  $\alpha$ -helix forms, 1:1) in the  $\beta$ -sheet form are 19, 20 and 21 ms, respectively. On the other hand, the  $^1\text{H } T_{1\rho}$  values determined from the C $\alpha$ , C $\beta$ , C $\gamma$  and C=O carbons of pure PLV in the  $\beta$ -sheet form are 19, 18, 18 and 19 ms, respectively. The  $^1\text{H } T_{1\rho}$  values for PLV with the  $\beta$ -sheet form and PLA in the  $\beta$ -sheet form are very close to each other. However, the  $^1\text{H } T_{1\rho}$  values for PDA in the  $\alpha$ -helix form are larger than those for PLA and PLV in the  $\beta$ -sheet form. In the PDA/PLV (50/50) blend, the  $^1\text{H } T_{1\rho}$  values determined from the C $\alpha$ , C $\beta$  and C $\gamma$  carbons of PLV in the  $\beta$ -sheet form are 16, 16 and 16 ms, respectively, and are thus slightly smaller than those for pure PLV. The  $^1\text{H } T_{1\rho}$  values determined from the C $\alpha$  and C $\beta$  carbons of PDA in the  $\alpha$ -helix form are 20 and 19 ms, respectively, and for the C $\alpha$  and C $\beta$  carbons of PDA in the  $\beta$ -sheet form they are 18 and 17 ms, respectively. These  $^1\text{H } T_{1\rho}$  values are approximately equal to each other. This shows that proton spin-diffusion between the PDAs in the  $\alpha$ -helix and  $\beta$ -sheet forms and PLV in the  $\beta$ -sheet form occurs on the  $^1\text{H } T_{1\rho}$  time scale.

The maximum effective diffusion distance was obtained from these  $^1\text{H } T_{1\rho}$  values. The maximum effective diffusion distance *L* of the proton spin-diffusion,  $D_{\text{spin}}$ , is expressed by the following equation [24]

$$L = (6D_{\text{spin}}t)^{1/2} \quad (1)$$

where  $D_{\text{spin}}$  is the spin-diffusion coefficient and in this work  $^1\text{H } T_{1\rho}$  is used for *t*. Although the value of  $D_{\text{spin}}$  may somewhat depend on the different proton densities in the blend systems, the average  $D_{\text{spin}}$  has been used in analysis of

Table 7  
Averaged  $^1\text{H}$   $T_{1\rho}$  values and  $L$  of polypeptide blend samples

Blend samples	$^1\text{H}$ $T_{1\rho}$ (ms) <sup>a</sup>	$L$ (nm)
PLA/PLIL (50/50)	16	3.1
PG/PLV (50/50)	15	3.0
PDA/PLV (50/50)	18	3.3

<sup>a</sup>  $^1\text{H}$   $T_{1\rho}$  value averaged over all of the protons.

polymer blend systems. In general, in the  $T_{1\rho}$  experiments on polymer blends the  $10^{-12}$  cm<sup>2</sup>/s as the averaged value has been used for determining qualitatively or semi-quantitatively the domain size of the blend systems [24]. By substituting the  $^1\text{H}$   $T_{1\rho}$  values averaged over all of the protons for PLA/PLIL (50/50), PG/PLV (50/50) and the PDA/PLV (50/50) blend samples into Eq. (1), we can approximately estimate  $L$  to be about 3 nm as the domain size (Table 7). This shows that the domain size of the individual polypeptides in the blend is not so large, and they are miscible at the molecular level. It can be said that this equation should be used for qualitative or semi-quantitative discussion of the miscibility of polymer blends as suggested by many reports [24].

We note that PLA with the  $\beta$ -sheet form in the PLA/PLIL blends is incorporated into PLIL in the  $\beta$ -sheet form and then takes the  $\beta$ -sheet form by forming hydrogen bonds with PLIL. However, the other component of PLA takes the  $\alpha$ -helix form. In addition, proton spin-diffusion between the PLAs in the  $\alpha$ -helix and  $\beta$ -sheet forms and PLIL in the  $\beta$ -sheet form occurs on the  $^1\text{H}$   $T_{1\rho}$  time scale and so PLA and PLIL are miscible at the molecular level with a domain size of about 3 nm. The other two kinds of PG/PLV and PDA/PLV blend samples, are miscible at the molecular level with a domain size of about 3 nm.

Finally, we observe that the polypeptides (PLA, PG and PDA) in the  $\beta$ -sheet form in the blend samples are incorporated into the polypeptides (PLIL and PLV) in the  $\beta$ -sheet form and then takes the  $\beta$ -sheet form by forming hydrogen bonds with the  $\beta$ -sheet form polypeptides (PLIL and PLV). In addition, proton spin-diffusion between the polypeptides (PLA, PG and PDA) in the  $\alpha$ -helix,  $3_1$ -helix and  $\beta$ -sheet forms and another component of the polypeptides (PLIL and PLV) in the  $\beta$ -sheet form occurs on the  $^1\text{H}$   $T_{1\rho}$  time scale and so blend samples are miscible at the molecular level with a domain size of about 3 nm.

## Acknowledgements

We thank Drs Toshimasa Yamazaki and Etsuko Katoh of

the National Institute of Agrobiological Sciences for helpful discussions.

## References

- [1] Karson RH, Norland kS, Fasman GD, Bluot ER. *J Am Chem Soc* 1960;62:2268.
- [2] Malcom BR. *Biopolymers* 1970;9:911.
- [3] Kiyotami H, Kanetsuna H. *J Polym Sci, Polym Phys* 1972;10:1931.
- [4] Saito H, Tabeta R, Ando I, Ozaki T, Shoji A. *Chem Lett* 1983;1437.
- [5] Okabe M, Yamanobe T, Komoto T, Watanabe J, Ando I. *J Mol Struct* 1989;213:213.
- [6] Akieda T, Mimura H, Kuroki S, Kurosu H, Ando I. *Macromolecules* 1992;25:5794.
- [7] Nakano J, Kuroki S, Ando I, Kameda T, Kurosu H, Ozaki T, Shoji A. *Biopolymers* 2000;54:81.
- [8] Andries JC, Anderson JM, Walton AG. *Biopolymers* 1971;10:1049.
- [9] Saito H, Tabeta R, Shoji A, Ozaki T, Ando I, Miyata T. *Biopolymers* 1984;23:2279.
- [10] Saito H, Tabeta R, Asakura T, Iwanaga Y, Shoji A, Ozaki T, Ando I. *Macromolecules* 1984;17:1405.
- [11] Ando S, Yamanobe T, Ando I, Shoji A, Ozaki T, Tabeta R, Saito H. *J Am Chem Soc* 1985;107:7648.
- [12] Murata K, Shigeki K, Kimura H, Ando I. *Biopolymers* 2002;64:26.
- [13] Saito H, Tabeta R, Shoji A, Ando I, Asakura T. In: Govil G, Khetrpal CL, Saran A, editors. *Magnetic resonance in biology and medicine*. New Delhi: Tata McGraw Hill; 1985. p. 195.
- [14] Saito H, Ando I. *Annu Rep NMR Spectrosc* 1989;21:210.
- [15] Ando I, Yamanobe T, Asakawa N. *Prog NMR Spectrosc* 1990;22:349.
- [16] Shoji A, Ando S, Kuroki S, Ando I, Webb GA. *Annu Rep NMR Spectrosc* 1993;26:55.
- [17] Asakawa N, Kameda T, Kuroki S, Kurosu H, Ando S, Ando I, Shoji A. *Annu Rep NMR Spectrosc* 1998;35:55.
- [18] Ando I, Asakura T, editors. *Solid state NMR of polymers*; 1998. p. 819.
- [19] Wei F, Lee D, Ramamoorthy A. *J Am Chem Soc* 2001;123:6118.
- [20] Lee D, Ramamoorthy A. *J Phys Chem B* 1999;103:271.
- [21] Kameda T, Asakura T. *Annu Rep NMR Spectrosc* 2002;46:101.
- [22] Saito H, Tabeta R, Shoji A, Ozaki T, Ando I. *Macromolecules* 1983; 16:1050.
- [23] Fasman GD. *Poly- $\alpha$ -amino acid*. New York: Marcel Dekker; 1967. chapter 11.
- [24] Asano A, Takegoshi K. In: Ando I, Asakura T, editors. *Solid state NMR of polymers*. Amsterdam: Elsevier; 1998. Chapter 10.
- [25] Yoshimizu H, Ando I. *Macromolecules* 1990;23:2908.
- [26] Yoshimizu H, Mimura H, Ando I. *Macromolecules* 1991;24:862.
- [27] Yoshimizu H, Mimura H, Ando I. *J Mol Struct* 1991;246:367.
- [28] Mueller D, Kricheldorf RH. *Polym Bull* 1981;6:101.
- [29] Taki T, Yamashita S, Satoh S, Shibata A, Yamashita T, Tabeta R, Saito H. *Chem Lett* 1981;1803.
- [30] Ando I, Saito H, Tabeta R, Shoji A, Ozaki T. *Macromolecules* 1984; 17:457.
- [31] Zhang X, Takegoshi K, Hikichi K. *Polym J* 1991;23:87.
- [32] Tang P, Reimer JA, Denn MM. *Macromolecules* 1993;26:4269.
- [33] Guo M. *TRIP* 1996;4:238.
- [34] Schantz S. *Macromolecules* 1997;30:1419.
- [35] Assink RA. *Macromolecules* 1978;11:1233.